# RAPID-MOLT: A Meso-scale, Open-source, Low-cost Testbed for Robot Assisted Precision Irrigation and Delivery

Marius Wiggert*[1], Leela Amladi*[1], Ron Berenstein[1], Stefano Carpin[2], Joshua Viers[3], Stavros Vougioukas[4], Ken Goldberg[1]

***Abstract*— To study the automation of plant-level precision irrigation, specifically learning-based irrigation controllers, we present a modular, open-source testbed that enables real-time, fine-grained data collection and irrigation actuation. RAPID-MOLT costs USD $\$600$ and has floor space of $0.37\mathrm{m}^2$. The functionality of the platform is evaluated by measuring the correlation between plant growth (Leaf Area Index) and water stress (Crop Water Stress Index) with irrigation volume. In line with biological studies, the observed plant growth is positively correlated with irrigation volume while water stress is negatively correlated. Construction directions, experimental data, CAD models, and related software are available at github.com/BerkeleyAutomation/RAPID-MOLT.**

## I. Introduction

Precision irrigation aims to optimize water usage, crop yield, and crop quality. This field has gained momentum in recent years as concerns over efficient use of water resources and groundwater contamination grow. In areas with more than 40% of the worlds population, global water demand already surpasses supply, and agricultural irrigation places the largest strain on this dwindling resource as it accounts for about 75% of the world's managed freshwater supply [1], [2]. However, plants absorb only between 5% to 30% of this water [2]. As a result of over-watering, nitrate fertilizers leach back into groundwater, thereby contaminating freshwater sources [3]. Moreover, crop yield and quality are not directly correlated to irrigation volume beyond a certain level. For many plants, including grapes, maintaining a crop water deficit has been shown to produce higher quality yield [4].

To optimize for Water Use Efficiency (WUE) and plant yield at scale, precision agriculture focuses on three key components: (1) affordable remote sensing, (2) spatially variable irrigation actuation, and (3) robust, adaptive irrigation controllers. Promising research is being conducted on remote sensing methods, such as Unmanned Aerial Vehicle (UAV) based multispectral imaging [5] and soil moisture sensors. The Robot Assisted Precision Irrigation Delivery (RAPID) project has focused on the delivery of per-plant, precise irrigation with a co-robotic approach for adjusting irrigation emitters [6]. Efficient irrigation policies that consider data such as crop phenotype, growth stage, leaf area, soil and field characteristics, and climate conditions have also been studied [7].

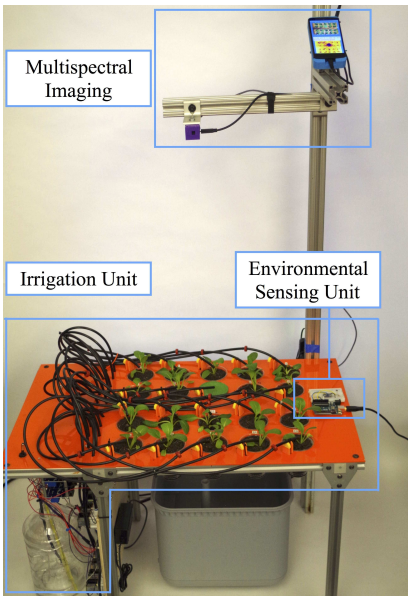


Fig. 1. The RAPID-MOLT with a sensing unit consisting of environmental sensing, multispectral imaging, and an actuation unit in which 20 solenoids can deliver different variable irrigation rates to 20 pots. Sensing and actuation is controlled with an Arduino Uno and Raspberry Pi.

However, crop irrigation simulators and applied control approaches have largely focused on zone-level instead of plant-level irrigation schedules. Thus, although spatially and temporally dense multispectral image sensing can provide very localized plant data, limited work has applied this to precision irrigation.

We present a low-cost, open-source, experimental testbed to study the potential for automating plant-level precision irrigation controllers. The contributions are as follows:

1) A hardware system design that enables both plant level sensing with multispectral imaging and also precise irrigation control with Raspberry Pi actuated solenoids.
2) A software infrastructure and data processing pipeline to evaluate irrigation controllers, including the automatic extraction of Leaf Area Index and Crop Water Stress Index from RGB and thermal images.
3) Data from two experiments with different plants, measuring plant growth and water stress data in response to different irrigation schedules.

*These authors contributed equally to the paper.
[1]The AUTOLab at UC Berkeley (automation.berkeley.edu) {mariuswiggert, leelaamladi, ron.berenstein, goldberg}@berkeley.edu; [2] School of Engineering, UC Merced scarpin@ucmerced.edu; [3]Center for Watershed Sciences, UC Merced, jviers@ucmerced.edu; [4] Biological and Agricultural Engineering, UC Davis, svougioukas@ucdavis.edu

## II. Related Work

### A. Existing Platforms for Precision Agriculture

There are several existing platforms with features required for irrigation control. The Farmbot is a CNC style mechanism that consists of a plot for plants and a modular set of interchangeable tools [8]. The tools can execute a variety of tasks including soil moisture sensing, RGB imaging, planting, weeding, and irrigating. The platform is completely open-source, with users encouraged to develop their own tools. The basic assembly kit is priced at USD $\$2,595$. Tencent and Wageningen University's "Greenhouse Competition" challenged researchers to develop irrigation controllers with which to autonomously cultivate cucumbers for four months inside a greenhouse [9]. Teams provided their own sensors and cameras with which to collect plant and environmental data. While this competition provides researchers with a platform to deploy experimental models, these platforms are not open-source for the community to utilize and build upon. Finally, as the internet of things expands, products providing smart irrigation have multiplied. However many of these products rely either on manual timer adjustment; such as products from Claber and Oysir; or on weather trends, such as products from Rachio, RainMachine, and Netro [10], [11], [12], [13], [14], [15]. While these options offer great utility to the average home grower, they do not enable plant-level control.

### B. Remote plant and Environmental Sensing

Environmental and crop data collection has seen an explosion of remote sensing technologies, including soil moisture sensing, multispectral sensing, in which images can be acquired over many wavelengths, and the use of RF waves in existing Wi-Fi bands [16]. These methods serve as proxies for conventional, manual methods of crop water status assessment such as leaf conductance and stem potential [17]. Direct soil moisture sensing data must be extracted from multiple physical sensors, and data resolution is heavily dependent on the number of sensors available [15].

Multispectral sensing as deployed through local, UAV, or satellite imaging, has potential to be proxy for manual, ground-truth measurements of parameters such as leaf conductance, stem potential, and root potential predictions [4]. These methods offer plant-level precision data without the cost of additional sensor installation, and could be used to data on both plant and environmental states including parameters such as Crop Water Stress Index (CWSI), Leaf Area Index (LAI), soil temperature, and canopy chlorophyll index. Multispectral technology has also been used in monitoring plant diseases, pests, and the spread of invasive plant species; estimating crop yield; and finely classifying crop distributions [18]. As of 2016, the agricultural market for drones alone was estimated at a value of USD $500 billion [19]. Private satellite companies such as Planet or HyperSat LLC are developing services that deliver daily global multispectral imaging to a variety of industries [20], [21]. As the commercial options for multispectral imaging are expanding, we chose it as the primary method of precision sensing for the Meso-Scale, Open-Source, Low-Cost Testbed (RAPID-MOLT) system.

### C. Plant State Characterization

The success of multispectral imaging is due to the establishment of multiple canopy temperature based proxies for plant water state measurements (leaf conductance or stem potential). Early research discovering a linear relationship between leaf-air temperature difference and vapor pressure deficit, the difference between current air moisture and air moisture at saturation, laid the groundwork for using leaf temperature for irrigation scheduling [22]. Three different temperature indices followed: Stress Degree Day (SDD), the canopy-air temperature difference measured at the time of maximum heat, Temperature Stress Day (TSD), the difference in canopy temperatures between stressed crop and non-stressed reference crop, and Critical Temperature Variability (CTV), the range of temperatures measured in a plot [23]. Each of these indices were shown to be unreliable or impractical for a variety of reasons: Gardner et al. demonstrated that stressed corn plants were mostly below air temperature confirming that a negative SDD is not enough to accurately signal water stress, TSD requires that a non-stressed reference plot be maintained near a testing site, and the selection of a critical CTV value relies on soil variability, which is difficult to quantify [23], [24].

The shortcomings of these indices led researchers to derive a new index, CWSI, from a combined energy balance-aerodynamic relation used to predict evaporation from natural surfaces [25]–[28]:

$$CWSI = \frac{T_{leaf} - T_{wet}}{T_{dry} - T_{wet}} \tag{1}$$

where $T_{leaf}$ is the leaf temperature measured, $T_{wet}$ is the leaf temperature of a well-watered, non-stressed plant leaf, and $T_{dry}$ is the temperature of a reference plant leaf with no transpiration. Meron et al. further simplified the index by estimating $T_{wet}$ using a Wet Artificial Reference Surface (WARS) instead of a non-stressed reference plant, and, as proposed in earlier studies, by estimating $T_{dry}$ as follows [29], [30].

$$T_{dry} = T_{air} + 5°C \tag{2}$$

In 2007, Moller et al. compared these approximations of $T_{dry}$ and $T_{wet}$ to other suggested approximation methods, and found the highest degree of correlation between leaf conductance and CWSI with the use of Equation 2 and a WARS [4]. For this, $T_{leaf}$ was gathered through RGB masking of canopy thermal images [4].

In addition to parameters characterizing water state, indices representing growth have also been developed for remote sensing technologies. The most widely used parameter is the Leaf Area Index $LAI = \frac{A_{leaf}}{Aground}$, a dimensionless ratio of the one sided leaf area, $A_{leaf}$, per ground area, $A_{ground}$ [31].

For RAPID-MOLT we use Equations 1 and 2 to measure crop water stress and $LAI$ to characterize plant growth.

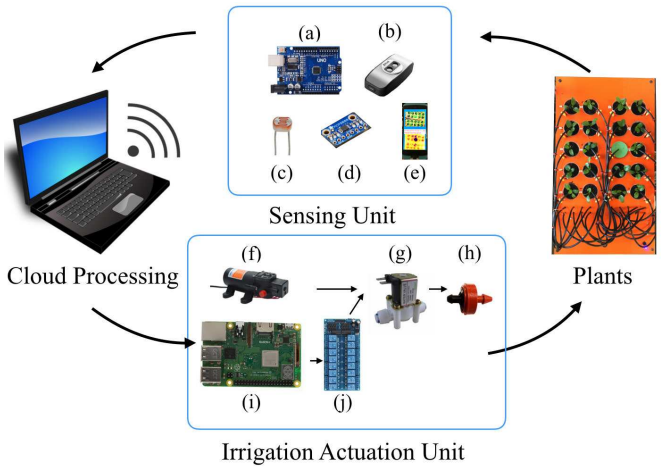


Fig. 2. Data and Irrigation flow. The sensing unit consists of (a) an Arduino Uno, (b) FLIR One Gen 2 Dual RGB/Thermal Camera, (c) light dependent resistor, (d) ambient Temperature Sensor, and (e) Android phone (Google Nexus 5) to collect FLIR images and upload to the cloud. Data can be used to adjust irrigation scheduling, which is executed by the Raspberry Pi. The irrigation unit consists of (f) one water pump, (g) 20 solenoids, (h) 20 drip emitters, (i) one Raspberry Pi, and (j) 20 electrical relays.

### D. Variable Irrigation Delivery

The RAPID project is investigating plant-level adjustable drip emitters as well as a robotic platform and routing algorithms for their efficient adjustment in the field [6], [32]–[35]. However, the majority of work into irrigation deployment has focused on zone-level, where, for simplicity, the soil and plant states inside of a large zone are assumed to be homogeneous. Variable rate pivot irrigation is one instance of this [36]. Here, crops are irrigated by sprinklers that rotate about a pivot at a rate that adjusts to incoming precision sensing data. The sprinkler, designed to maximize the number of crops reached at once, delivers zone-level irrigation, and it is thus difficult to predict the volume of water that each plant is receiving. The lack of low-cost, open-source platforms for precision irrigation delivery is a key missing link in researchers' efforts to develop robust irrigation controllers and motivates the development of RAPID-MOLT.

## III. Design

### A. Motivation and Design Considerations

A research platform conducive to the development of precise irrigation controllers requires both precision sensing and methods for precision irrigation deployment. Additional objectives are as follows: (1) low unit cost, (2) meso-scale platform size to fit an indoor laboratory setting, (3) maximized number of pots to enable the collection of a large and varied dataset, (4) data that can be remotely accessed and processed, and (5) open-source documentation. The following sections detail how the platform was designed for each objective.

### B. Hardware Design

RAPID-MOLT consists of the (1) Frame holding the plant pots, (2) Sensing Unit, and (3) Irrigation Unit (Figure 3).

TABLE I
RAPID-MOLT Components Cost and Specifications.
Total cost is USD $610

| Item | Cost [USD$] | Specs |
|---|---|---|
| 1x FLIR One Gen 2 | 250.00 | Thermal Resolution: 160x120<br>RGB Resolution: 640x480<br>Sensitivity: 0.1°C<br>Spectral range: 8 to 14m<br>Field of View: 46°x 35° |
| 20x Solenoid | 149.80 | 12V |
| 1x Google Nexus 5 | 100.00 | Display Size: 126 mm<br>Display Resolution: 10801920 pixels |
| 1x Raspberry Pi | 31.10 | Lan Speed: 10/100Mbps<br>No. USB ports: 4<br>No. GPIO pins: 40 |
| 1x Arduino Uno | 21.43 | Operating Voltage: 5V<br>Microcontroller: ATmega328P |
| 1x Water Pump | 16.31 | 12 V, 4.3 L/min, 35 psi |
| 1x Relay* 16 channel | 14.99 | 12V |
| 20x Emitter | 9.68 | Flowrate: 0.5 gph<br>Pressure Range: 10 to 45 psi |
| 1x Relay* 8 channel | 8.59 | 5V |
| 1x Ambient Temperature Sensor | 4.95 | Accuracy: 0.25°C<br>Range: -40°C to +125°C<br>Precision: 0.0625°C. |
| 1x Light Dependent Resistor (LDR) | 0.17 | 0.6 Ohms/Lux<br>Spectral Range: 400 to 700 nm |

*Note: Two relay panels (8 channel and 16 channel) were combined to obtain the 20 channels necessary to have on relay per pot.

These units function together as shown in Figure 2.

The base is designed to minimize both cost and space and consists of a frame assembled from aluminum 8020 extrusion (0.812 x 0.457 x 1.600 m); an acrylic laser-cut top plate with forty through-holes, twenty for pots and twenty for stationary irrigation tubes; and a stationary mount for the Forward-Looking Infrared Radar (FLIR) camera. Stationary mounts were used to avoid large costs associated with the precision machining of a robust linear rail. The modular top plate is connected to the base with four mounting holes, and pot through-holes are sized at 70mm to support cups at the lip. Irrigation tube through-holes are sized at 6.35mm. Each of these dimensions can be easily modified to account for various amounts and types of pots and tubing, all contributing to the modularity of the system. For multispectral sensing, the FLIR One, Gen 2 dual RGB/Thermal camera is enclosed in a stationary camera mount. With our focus on precision irrigation, a thermal camera, which utilizes a far infrared spectrum, was chosen following its use in a plethora of studies showing temperature to be an accurate proxy for crop water status. A limitation of this low-cost model is that it must be paired with an Android phone, for which, the inexpensive Google Nexus 5 is selected. To fit the platform in the FLIR field of view, the camera is mounted 66cm above the top plate plane. Finally, disposable, clear plastic cups with a 72 mm opening diameter are selected as plant pots to further minimize cost. Cup transparency allows further investigation of the soil and seeds' growth during the growing cycle.

The Sensing Unit, Figure 2, consists of an ambient light sensor, ambient temperature sensor, Arduino Uno for the

collection of this ambient data, and a FLIR One Gen 2 dual RGB/Thermal camera for multispectral imaging of plant parameters. Ambient light data provides context on how sunlight affects temperature throughout data collection, and ambient temperature data is used to calculate $T_{dry}$ as required in Equations 1 and 2. The light sensor, with a relatively low sensitivity, provides us with ambient lighting trends rather than reliable magnitudes. Temperature and incident light data is collected with an Arduino Uno, but can also be collected with the Raspberry Pi that is controlling the actuation unit.

The Irrigation Unit, as shown in Figure 3 consists of a water pump, Raspberry Pi computer, one electric relay panel, solenoid actuator, and a low-flow drip emitter (1.9 liter/hour) for each of the twenty pots. Solenoid actuation is selected for variable irrigation deployment in line with its use in similar products such as the Farmbot. The low flow-rate emitters are used for their ability to deliver precise irrigation amounts. The Raspberry Pi, also the computer of choice for the Farmbot, is selected for its low-cost, connectivity capabilities, and its large open-source community. The water supply is routed from an external refillable container, through a solenoid actuator that is controlled by an electric relay. Sufficient pneumatic tubing is required for the routing of the water supply. Each relay is actuated by the Raspberry Pi, which can be set to autonomously respond to plant and environmental data that is collected by the sensing unit. Angled, 3D-printed, risers are placed at the exit of each irrigation tube to ensure proper tube fixation and delivery of water to each pot. Power must be supplied to the irrigation unit through a standard 110 V outlet.

For the frame, sensing unit, and actuation unit, each component is chosen to minimize overall platform cost while ensuring sufficient accuracy. Each component can be replaced with instruments of higher precision. Cost and specifications for each of the components are listed in Table I. Documentation detailing ordering information for each listed part is included on the project website.

### C. Software Design

The primary goal of the RAPID-MOLT software is a modular design to allow for the addition of sensors, the customization of the data processing, and the seamless implementation of different controllers. Therefore, the software is split into three parts: (1) the sensing software, (2) the data processing software, (3) the actuator control software.

*1) Sensing Software:* The sensing software consists of an Arduino script that logs ambient temperature and incident light readings (Figure 2.b, 2.c), and a simple Android application that uploads the resulting multispectral images to the cloud. The data acquisition and upload rates are configurable.

*2) Data Processing Software:* The data processing pipeline runs daily. Raw images and sensor data are downloaded from the cloud and archived locally. First, twenty circular masks are created to distinguish each pot. To create these masks, color thresholding of orange, the color of this specific platform's top plate, is executed in the Hue-Saturation-Intensity (HSV) color space to mask out the background. The pot mask is then cleaned in OpenCV using Morphological Transformations with circular structuring elements to detect individual pot contours and centers. Pot centers are then labeled and ordered according to a specified pot numbering system. A circle is drawn around each, resulting in 20 clean circular masks, one for each pot location as seen in Figure 4.

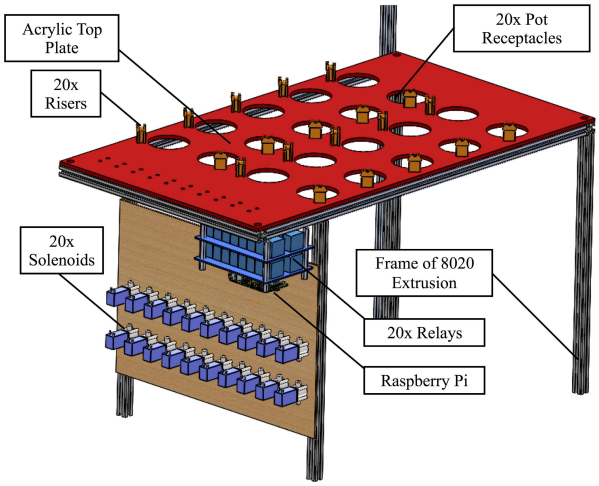


Fig. 3. CAD Model of the frame and irrigation delivery unit. The Raspberry Pi, water pump, 20 solenoids, and 16 and 8 channel relay panels are shown. Irrigation tubing and electrical wiring is omitted for better visualization.

Next, Leaf Area Index $LAI = \frac{A_{leaf}}{A_{ground}}$ (section II-C) which serves as our plant growth metric, is calculated from the RGB image [31]. For this, a second mask consisting only of the plant leaves is created by applying threshold values for the leaf color to the RGB image in the HSV color space. This plant leaf mask is intersected with each of the 20 pot masks computed in the previous step resulting in 20 pot-leaf masks. Based on these, the ratio of pixels corresponding to leaf surface to total pot pixels for each pot is calculated to obtain a reasonable approximation of the $LAI$. The process is visualized in Figure 4. Specific threshold values in the HSV color space are chosen once at the beginning of the experiment by manually inspecting masking results for images with different light conditions.

The twenty pot-leaf masks are then applied to the thermal images to extract all thermal image pixels corresponding to leaf surface pixels, as shown in Figure 4. The pot-specific leaf temperature, $T_{leaf}$, is determined by the median of the leaf-temperature-pixels. Pixel median was chosen for robustness to outliers that may be produced by imperfect masking.

Finally, plant state data ($T_{leaf}$ and $LAI$) is aligned with environmental state data collected by the Arduino Uno (ambient air temperature $T_{air}$ and incident light $L_{incident}$) based on time stamps. This comprehensive data is then available for an irrigation controller to determine a suitable irrigation schedule, in which irrigation is specified as seconds of solenoid actuation per plant. As water volume deployed

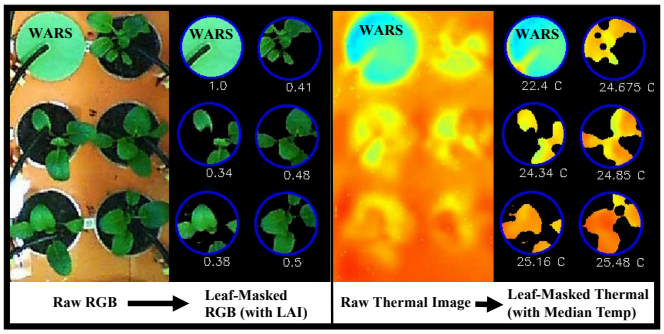


Fig. 4. The image processing pipeline from left to right for a subset of the platform with the wet reference surface (WARS) on the top left. Starting with the raw RGB, the leafs of the plants are masked and $LAI$ is calculated for each pot. The leaf mask is then applied to the raw thermal image and then for each pot the median temperature is taken as $T_{leaf}$.

is reliant on the duration of a solenoid actuation, a platform-specific calibration must be executed to relate these two quantities. The irrigation decision, specified in a csv file, can then be sent to the Raspberry Pi for execution.

*3) Actuation Software:* The actuation software on the Raspberry Pi executes the irrigation actuation by opening and closing the Solenoids at the right times. For the experiments minute scale sensing and daily actuation cycles are selected but this can be adjusted as desired.

### D. Limitations

As a result of the design objectives stated in Section III-A, the platform is subject to some inherent limitations. In attempting to both size the platform for an indoor laboratory setting as well as maximizing the number of individual pots, the size of the plants that can be grown is directly constrained. Additionally, the platform's dependence on one Raspberry Pi limits the number of available General Purpose Input/Output (GPIO) ports, and therefore testable pots, to twenty-six. To increase the number of pots the platform would require a GPIO expansion board and/or and additional Raspberry Pi. A third limitation experienced during image processing is the growth of plant leaves past pot diameters. Due to the pot masking only the leaves inside of pot are taken into account for both $LAI$ and $T_{leaf}$ measurement. To prevent this, pots should be spaced according to expected growth patterns of experimental plants used.

## IV. Evaluation Experiments

To evaluate the platform's ability to monitor individual plant growth and plant water stress, two experiments monitoring plant responses to varying levels of irrigation are conducted. Both plant growth and water stress are useful as feedback control signals for automated precision irrigation.

To characterize actuation error and determine the function of solenoid actuation (in seconds) to volume of water delivered (mL), a calibration test of the irrigation unit is conducted. To match the implemented range of 1s to 6s of solenoid actuation time, five runs are conducted at solenoid actuation times of 2s, 4s, and 6s. Output volumes are measured for each run. The average standard deviation of the output volumes is 0.1023 mL.

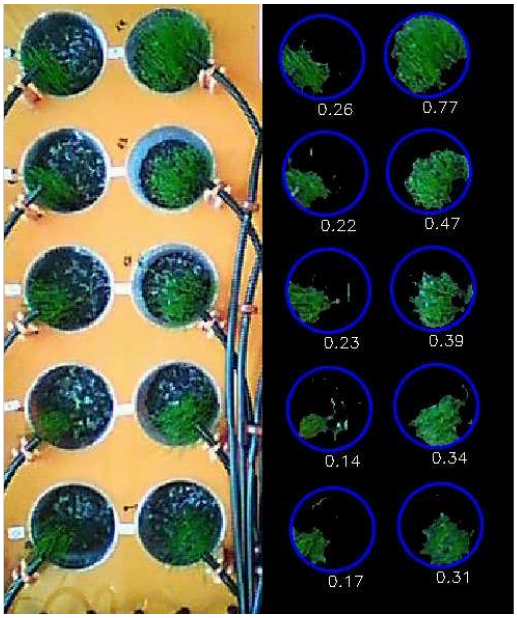


Fig. 5. Half of the RAPID-MOLT pots shown on the 8th day of the experiment monitoring grass growth under variable irrigation. The figure shows the raw RGB image (left side) from which the leaf masks and $LAI$ values for each pot (right side) are extracted. The bottom left pot received 0.72mL of irrigation, increasing up to 1.41mL for the top left, continuing with the second column upwards ending at 2.08mL at the middle top right pot. The right part shows the left RGB image processed via the data pipeline. As can be seen the $LAI$ values correlate positively with the daily applied irrigation input.

### A. Experiment 1: Monitoring Plant Growth

In the first experiment, crop growth under differential irrigation is monitored for two consecutive weeks. Nineteen pots are filled with a mixture of soil and 70 grass seeds of the type "Pennington Smart Seed Sun and Shade". Gras and specifically those seeds were selected for their fast germination and growth cycles which allow for swift evaluation of RAPID-MOLT's growth monitoring capability. All plants are potted with a 0.5 cm layer of stones placed above a hole in the pot bottom. This allows for the drainage of superfluous water but prevents the drainage of soil.

Different irrigation durations are applied to each pot, from a solenoid actuation per day of 1s up to 5.75s, with steps of 0.25s. This corresponds to irrigation volumes from 0.73 to 3.12 mL. Pots were irrigated at noon. Multispectral images, temperature, and incident light readings are taken every ten minutes for two consecutive weeks. Figure 5 shows an RGB image from the eighth day of the experiment labelled with $LAI$ values derived from the image processing pipeline detailed in section III-C.

As hourly measurements are noisy, only the daily median $LAI$ value is used, producing 19 $LAI$ measurements, one per pot, over 14 days (Figure IV-A). Noise in hourly measurements is largely due to changing light conditions that affect the thresholds for HSV filtering in the image processing pipeline.

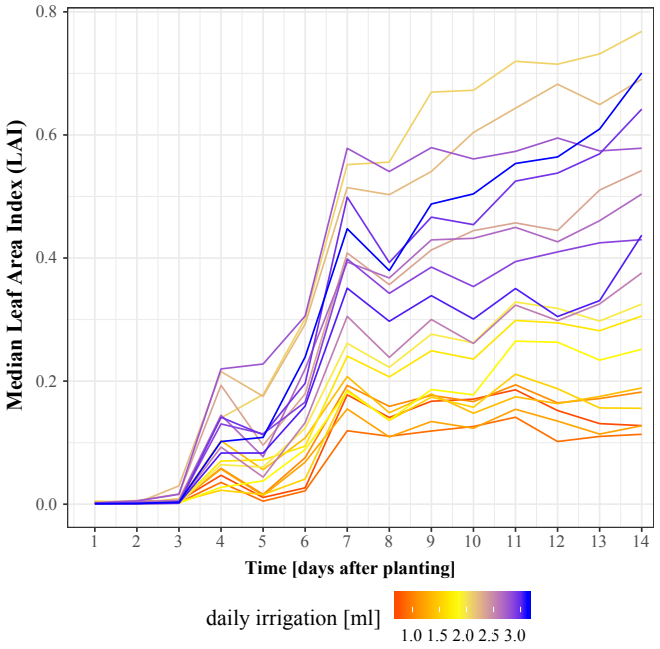


The colors indicate the different amounts of daily irrigation applied. We can see that little daily irrigation correlates with slower LAI growth.

The colors indicate the different amounts of daily irrigation applied. We can see that little daily irrigation correlates with slower LAI growth.

Fig. 6. This plot shows the development of the daily mean LAI of 19 pots with grass seeds planted on day 0 and different daily irrigation amounts. The LAI value, as proxy for plant growth, is obtained from the RGB image over the time of two weeks. Daily irrigation growth correlates with LAI growth, however exceptions occur as shown in upper right and discussed in the text.
The colors indicate the different amounts of daily irrigation applied. We can see that little daily irrigation correlates with slower LAI growth.

During the experiment, it was observed that grass germinated and sprouted on approximately the third day after planting, resulting in an increase of $LAI$. There onwards, plant growth rates ($LAI$) diverged, tracking their differential irrigation levels. This behavior matches general expectations of plant growth and also matched visual observations over the course of the experiment. Grass receiving the most irrigation grew to a $LAI$ of 0.75 over 14 days whereas the least irrigated grass pot achieved a $LAI$ of 0.12. The flattening of the $LAI$ growth curves toward the end of the experiment do not necessarily indicate slowing plant growth, and is likely results from the inherent limitation of top-view RGB imaging in which vertical leaf-growth is difficult to detect. Additionally, the $LAI$ curves in Figure IV-A are not increasing monotonically. Specifically, there are two jumps in $LAI$, seen on the fourth and seventh day. This is likely due to especially bright lighting conditions on those days, as observed when reviewing experimental data (similar to Figure 4).

While the experimental data shows a significant correlation of plant growth and daily irrigation volume, the $LAI$ curves in Figure IV-A are not strictly ordered according to irrigation volumes. One possible explanation is heterogeneous initial conditions, i.e. different amounts of soil and seeds between pots. Other sources of error could include natural fluctuations in seed germination rates, noise in the FLIR imaging, or imperfect $LAI$ extraction through the image processing pipeline. However, it is notable that even with homogeneous initial conditions, images devoid of noise, and perfect image processing, the plant growth would likely still vary due to different phenotypes in the biological populations.

$LAI$ provides a valuable signal for automated precision irrigation. To study the relationship between individual plant growth ($LAI$) and irrigation, further experiments with wider leaf plants are planned.

### *B. Experiment 2: Plant water stress response to irrigation*

In this experiment CWSI is measured for different irrigation amounts over six consecutive days. Nineteen Pak Choi seedlings (5cm tall) from the local plant nursery are used as the experimental crop due to their high water sensitivity and large leaf area as seen in Figure 4. One pot, designated as the WARS surface, is covered with two layers of a thin cotton cloth and irrigated every fifteen minutes for five seconds thereby providing the wet reference surface needed to measure $T_{wet}$ [29]. To reduce the uneven heating patterns induced by uneven direct sunlight, this experiment is performed without direct sunlight exposure. Each plant is watered sufficiently for two days prior to the experiment start so as to bring all nineteen plants to a standardized, non-stressed water state. The plants are randomly divided into three groups, to which the following different irrigation volumes (seconds of solenoid actuation time) are applied: $0\mathrm{ml}$ (0s, no irrigation), $2.85\mathrm{ml}$ (5s), $10.8\ \mathrm{ml}$ (20s). Plants are irrigated over six days, at 4:00pm each day. Multispectral images, temperature, and incident light readings are taken every 5 minutes to ensure temporally dense observations.

As shown in Figure 8, the initially equal CWSI of well watered plants (close to zero) changes depending on the applied irrigation schedule. While it is observed that both zero daily irrigation and limited daily irrigation causes an increase in CWSI, zero irrigation results in significantly more water stress (a higher CWSI). Daily irrigation of $10.8\ \mathrm{ml}$ of water produces a CWSI value that fluctuates around zero, signalling no water stress. These results are qualitatively comparable to results of a similar experiment conducted by biologists, where CWSI and ground truth water stress was measured with high-quality instruments [37]. In this 2002 experiment, well-watered plants were divided into one group that received zero irrigation, and another group that received sufficient irrigation to maintain soil moisture at 45% [37]. A similar increase in CWSI was observed for the water-stressed plants [37]. This parallel indicates that RAPID-MOLT's low-cost sensing hardware is sufficient to sense the water state of plants with significant leaf area. The fast CWSI response of plants to deficient irrigation suggests that its usefulness as feedback signal for irrigation automation.

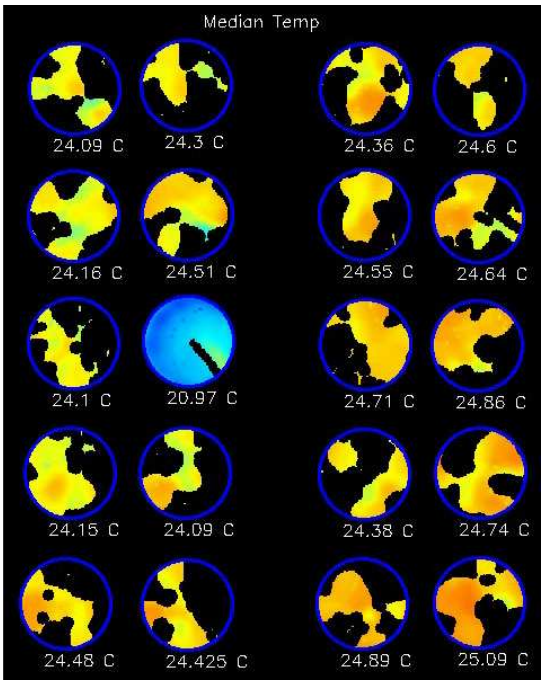


Fig. 7. The median temperatures $T_{leaf}$ of each pot shown at 3pm during our CWSI experiment with Pak Choi seedlings under three different irrigation schedules. There is a negative correlation between $T_{leaf}$ and the amount of irrigation applied to each plant, making $T_{leaf}$ range from $24.09°C$ $(0\frac{ml}{day})$ to $25.09°C$ $(10.8\frac{ml}{day})$

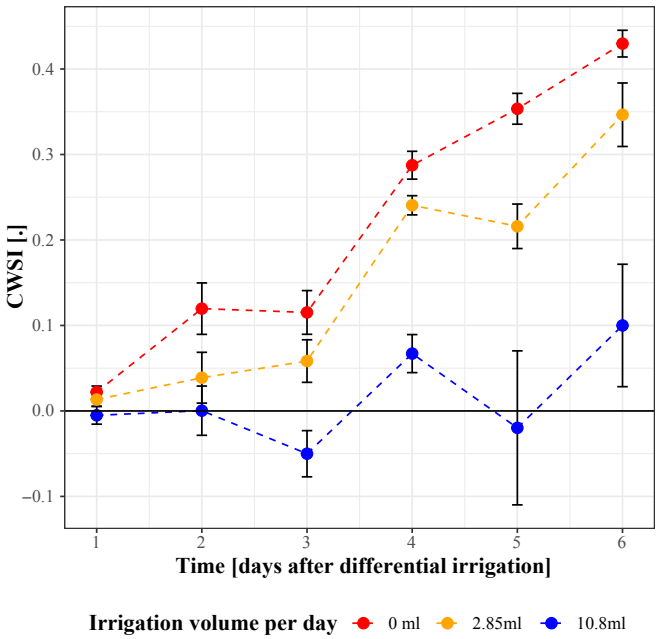


Fig. 8. This plot shows the development of CWSI for three groups of initially well-watered Pak Choi plants under different irrigation schedules over six days. Each point is the group mean CWSI value of the daily mean CWSI values of the six Pak Choi plants per group. The error bars indicate the standard error. Increasing water stress resulting from no/little irrigation is reflected in higher CWSI values.

## V. Summary and Future Work

We present an open-source, low-cost experimental testbed for the development and evaluation of plant-level, precision irrigation controllers. RAPID-MOLT's modular nature allows for the extension of platform capabilities through additional sensors, additional plants of potentially larger size, and algorithm customization at any layer of the software stack. A potential limitation of RAPID-MOLT is the quality of precision sensing data, drawn from a low-cost multispectral camera and ambient light and temperature sensors. It is notable that irrigation controllers must be robust to such noise as multispectral imaging from drones and satellites will likely contain noise as well.

As lighting conditions also significantly influence the opening and closing of stomata, thereby affecting $T_{leaf}$ and CWSI, future versions of RAPID-MOLT will include controllable lighting. This addition will directly decrease the sensitivity of RGB based $LAI$ measurements to lighting conditions. Initial evaluation results are promising and indicate that RAPID-MOLT can be used for the development of controllers that can adapt to variability in soil, environment, and plant conditions. Specifically, we aim to use learning-based controllers to be able to account for the complexity of interactions between environmental and plants states.

The CAD models, instructions, order information, component costs, and code is available at github.com/BerkeleyAutomation/RAPID-MOLT.

## Acknowledgment

This research was performed at the AUTOLAB at UC Berkeley in affiliation with the Berkeley AI Research (BAIR) Lab, Berkeley Deep Drive (BDD), the Real-Time Intelligent Secure Execution (RISE) Lab, and the CITRIS "People and Robots" (CPAR) Initiative, and by the RAPID: Robot-Assisted Precision Irrigation Delivery Project (USDA 2017-67021-25925 under NSF National Robotics Initiative). The authors were supported in part by donations from Siemens, Google, Amazon Robotics, Toyota Research Institute, Autodesk, ABB, Knapp, Loccioni, Honda, Intel, Comcast, Cisco, Hewlett-Packard and by equipment grants from PhotoNeo, NVidia, and Intuitive Surgical.

## References

[1] T. W. Bank, "Globally, 70% of Freshwater is Used for Agriculture," 2017. [Online]. Available: https://blogs.worldbank.org/opendata/chart-globally-70-freshwater-used-agriculture

[2] J. S. Wallace and P. J. Gregory, "Water resources and their use in food production systems," *Aquatic Sciences*, vol. 64, no. 4, pp. 363–375, 2002.

[3] X. P. Pang, J. Letey, and L. Wu, "Irrigation quantity and uniformity and nitrogen application effects on crop yield and nitrogen leaching," *Soil Science Society of America Journal*, vol. 61, no. 1, pp. 257–261, 1997.

[4] M. Mller, V. Alchanatis, Y. Cohen, M. Meron, J. Tsipris, A. Naor, V. Ostrovsky, M. Sprintsin, and S. Cohen, "Use of thermal and visible imagery for estimating crop water status of irrigated grapevine*," *Journal of Experimental Botany*, vol. 58, no. 4, pp. 827–838, 09 2006. [Online]. Available: https://dx.doi.org/10.1093/jxb/erl115

[5] L. Quebrajo, M. Perez-Ruiz, L. Pérez-Urrestarazu, G. Mart\'\inez, and G. Egea, "Linking thermal imaging and soil remote sensing to enhance irrigation management of sugar beet," *Biosystems Engineering*, vol. 165, pp. 77–87, 2018.

[6] R. Berenstein, R. Fox, S. McKinley, S. Carpin, and K. Goldberg, "Robustly adjusting indoor drip irrigation emitters with the toyota hsr robot," in *2018 IEEE International Conference on Robotics and Automation (ICRA)*. IEEE, 2018, pp. 2236–2243.

[7] R. Romero, J. L. Muriel, I. Garcia, and D. M. de la Peña, "Research on automatic irrigation control: State of the art and recent results," *Agricultural water management*, vol. 114, pp. 59–66, 2012.

[8] "Open-source cnc farming." [Online]. Available: https://farm.bot/

[9] "Autonomous green house challenge." [Online]. Available: http://www.autonomousgreenhouses.com/

[10] "Claber 8053 oasis 4-programs/20 plants garden automatic drip watering system." [Online]. Available: https://www.amazon.com/Claber-8053-4-Programs-Automatic-Watering/dp/B000U5YFR4/

[11] "Oysir automatic drip irrigation kit,self watering system timer irrigation controller indoor plant auto watering planter pot with usb for indoor plants." [Online]. Available: https://www.amazon.com/OYSIR-Automatic-Irrigation-Watering-Controller/dp/B07L5HT3CB/

[12] G. E. LLC, "Forecast smart wi-fi irrigation controllers." [Online]. Available: https://www.rainmachine.com/

[13] "The next wave of watering precision." [Online]. Available: https://www.rachio.com/

[14] "Your smarter home irrigation controller." [Online]. Available: https://netrogarden.com/

[15] N. Zhang, M. Wang, and N. Wang, "Precision agriculturea worldwide overview," *Computers and electronics in agriculture*, vol. 36, no. 2-3, pp. 113–132, 2002.

[16] F. Ozcep, E. Yıldırım, O. Tezel, M. Asci, and S. Karabulut, "Correlation between electrical resistivity and soil-water content based artificial intelligent techniques," *International Journal of Physical Sciences*, vol. 5, no. 1, pp. 47–56, 2010.

[17] Y. Osakabe, K. Osakabe, K. Shinozaki, and L.-S. P. Tran, "Response of plants to water stress," *Frontiers in Plant Science*, vol. 5, no. March, pp. 1–8, 2014. [Online]. Available: http://journal.frontiersin.org/article/10.3389/fpls.2014.00086/abstract

[18] M. Teke, H. S. Deveci, O. Haliloğlu, S. Z. Gürbüz, and U. Sakarya, "A short survey of hyperspectral remote sensing applications in agriculture," in *2013 6th International Conference on Recent Advances in Space Technologies (RAST)*. IEEE, 2013, pp. 171–176.

[19] G. Sylvester, "E-agriculture in action: Drones for agriculture," *Published by Food and Agriculture Organization of the United Nations and International Telecommunication Union, Bangkok*, 2018.

[20] "Home," May 2018. [Online]. Available: https://www.planet.com/

[21] H. LLC, "Hypersat llc to launch world's first commercial constellation of high-resolution hyperspectral imaging satellites in 2020 english latin america - espaol brazil - portugus franais nederlands deutsch," Sep 2018. [Online]. Available: https://www.prnewswire.com/news-releases/hypersat-llc-to-launch-worlds-first-commercial-constellation-of-high\-resolution-hyperspectral-imaging-satellites-in-2020-300712831.html

[22] W. L. Ehrler, "Cotton leaf temperatures as related to soil water depletion and meteorological factors 1," *Agronomy Journal*, vol. 65, no. 3, pp. 404–409, 1973.

[23] R. D. Jackson, "Canopy temperature and crop water stress," in *Advances in irrigation*. Elsevier, 1982, vol. 1, pp. 43–85.

[24] B. Gardner, B. Blad, R. Maurer, and D. Watts, "Relationship between crop temperature and the physiological and phenological development of differentially irrigated corn 1," *Agronomy journal*, vol. 73, no. 4, pp. 743–747, 1981.

[25] H. L. Penman, "Natural evaporation from open water, bare soil and grass," *Proceedings of the Royal Society of London. Series A. Mathematical and Physical Sciences*, vol. 193, no. 1032, pp. 120–145, 1948.

[26] R. D. Jackson, S. Idso, R. Reginato, and P. Pinter Jr, "Canopy temperature as a crop water stress indicator," *Water resources research*, vol. 17, no. 4, pp. 1133–1138, 1981.

[27] S. Idso, R. Reginato, R. Jackson, and j. P. Pinter, "Measuring yield-reducing plant water potential depressions in wheat by infrared thermometry," *Irrigation Science*, vol. 2, no. 4, pp. 205–212, 1981.

[28] R. Jackson, P. Pinter Jr, R. Reginato, and S. Idso, "Hand-held radiometry, usda-sea, agric. rev. and manuals," ARM-W-19, Tech. Rep., 1980.

[29] M. Meron, J. Tsipris, and D. Charitt, "Remote mapping of crop water status to assess spatial variability of crop stress," in *Precision agriculture. Proceedings of the fourth European conference on precision agriculture. Academic Publishers, Berlin*, 2003, pp. 405–410.

[30] S. Irmak, D. Z. Haman, and R. Bastug, "Determination of crop water stress index for irrigation timing and yield estimation of corn," *Agronomy Journal*, vol. 92, no. 6, pp. 1221–1227, 2000.

[31] D. J. Watson, "Comparative physiological studies on the growth of field crops: I. variation in net assimilation rate and leaf area between species and varieties, and within and between years," *Annals of botany*, vol. 11, no. 41, pp. 41–76, 1947.

[32] R. Berenstein, A. Wallach, P. E. Moudio, P. Cuellar, and K. Goldberg, "An open-access passive modular tool changing system for mobile manipulation robots," in *2018 IEEE 14th International Conference on Automation Science and Engineering (CASE)*. IEEE, 2018, pp. 592–598.

[33] D. V. Gealy, S. McKinley, M. Guo, L. Miller, S. Vougioukas, J. Viers, S. Carpin, and K. Goldberg, "Date: A handheld co-robotic device for automated tuning of emitters to enable precision irrigation," in *2016 IEEE International Conference on Automation Science and Engineering (CASE)*. IEEE, 2016, pp. 922–927.

[34] T. C. Thayer, S. Vougioukas, K. Goldberg, and S. Carpin, "Multi-robot routing algorithms for robots operating in vineyards," in *2018 IEEE 14th International Conference on Automation Science and Engineering (CASE)*. IEEE, 2018, pp. 14–21.

[35] D. Tseng, D. Wang, C. Chen, L. Miller, W. Song, J. Viers, S. Vougioukas, S. Carpin, J. A. Ojea, and K. Goldberg, "Towards automating precision irrigation: Deep learning to infer local soil moisture conditions from synthetic aerial agricultural images," in *2018 IEEE 14th International Conference on Automation Science and Engineering (CASE)*. IEEE, 2018, pp. 284–291.

[36] C. Perry, S. Pocknee, and O. Hansen, "A variable rate pivot irrigation control system," in *Proceedings of the Fourth European Conference in Presicion Agriculture*, 2003, pp. 539–544.

[37] M. Kacira, P. P. Ling, and T. H. Short, "Establishing crop water stress index (cwsi) threshold values for early, non–contact detection of plant water stress," *Transactions of the ASAE*, vol. 45, no. 3, p. 775, 2002.